

Thermoelectric properties of $\text{Ni}_{0.15}\text{Co}_{3.85}\text{Sb}_{12}$ and $\text{Fe}_{0.2}\text{Ni}_{0.15}\text{Co}_{3.65}\text{Sb}_{12}$ skutterudites prepared by HPHT method

LINGJIAO KONG¹, HONGAN MA^{1,*}, YUEWEN ZHANG¹, XIN GUO², BING SUN¹, BINWU LIU¹,
HAIQIANG LIU¹, BAOMIN LIU¹, JIAXIANG CHEN¹, XIAOPENG JIA¹

¹National Key Lab of Superhard Materials, Jilin University, Changchun 130012, China

²Institute of Materials Science and Engineering, Changchun University of Science and Technology, Changchun 130022, China

N-type polycrystalline skutterudite compounds $\text{Ni}_{0.15}\text{Co}_{3.85}\text{Sb}_{12}$ and $\text{Fe}_{0.2}\text{Ni}_{0.15}\text{Co}_{3.65}\text{Sb}_{12}$ with the bcc crystal structure were synthesized by high pressure and high temperature (HPHT) method. The synthesis time was sharply reduced to approximately half an hour. Typical microstructures connected with lattice deformations and dislocations were incorporated in the samples of $\text{Ni}_{0.15}\text{Co}_{3.85}\text{Sb}_{12}$ and $\text{Fe}_{0.2}\text{Ni}_{0.15}\text{Co}_{3.65}\text{Sb}_{12}$ after HPHT. Electrical and thermal transport properties were meticulously researched in the temperature range of 300 K to 700 K. The $\text{Fe}_{0.2}\text{Ni}_{0.15}\text{Co}_{3.65}\text{Sb}_{12}$ sample shows a lower thermal conductivity than that of $\text{Ni}_{0.15}\text{Co}_{3.85}\text{Sb}_{12}$. The dimensionless thermoelectric figure-of-merit (zT) reaches the maximal values of 0.52 and 0.35 at 600 K and 700 K respectively, for $\text{Ni}_{0.15}\text{Co}_{3.85}\text{Sb}_{12}$ and $\text{Fe}_{0.2}\text{Ni}_{0.15}\text{Co}_{3.65}\text{Sb}_{12}$ samples synthesized at 1 GPa.

Keywords: *thermoelectric materials; Fe-doping; skutterudite; high pressure*

1. Introduction

Thermoelectric (TE) materials with unexceptionable transport properties have recently been a subject of continuous interest and attention [1–3]. The performance of TE materials is generally characterized by the dimensionless figure-of-merit [4, 5]:

$$zT = S^2\sigma T/\kappa \quad (1)$$

where S , σ , T , and κ represent the Seebeck coefficient, electrical conductivity, absolute temperature, and total thermal conductivity, respectively. The $S^2\sigma$ is defined as the power factor. Skutterudite compounds have traditionally been known as the “phonon-glass and electron-crystal” (PGEC) concept that was introduced by Slack et al. [6] in 1995, in which the thermoelectric material has both a crystalline structure to ensure good electron transportation and a glass structure to reduce thermal conduction by enhancing phonon scattering. Although pure CoSb_3 does not exhibit excellent

thermoelectric performance because of the higher thermal conductivity, skutterudite compounds are expected to be the most promising TE materials due to numerous possibilities for modifications of thermoelectric properties, through substituting and/or filling of structural voids [7]. For example, Te substitution for Sb [8], Fe substitution for Co [9], and rare earth metals filling CoSb_3 [10] have been extensively researched to reduce thermal conductivity.

Compared with other methods, high pressure and high temperature (HPHT) method is a prospective synthesis technique for thermoelectric materials fabrication [11]. HPHT method has many advantages, such as the ability to tune rapidly, typically without introducing disorder. In addition, the synthesis time is shortened greatly to around half an hour. The method has been successfully applied to synthesize various thermoelectric materials [12].

In this article, $\text{Ni}_{0.15}\text{Co}_{3.85}\text{Sb}_{12}$ [13] and $\text{Fe}_{0.2}\text{Ni}_{0.15}\text{Co}_{3.65}\text{Sb}_{12}$ skutterudites were successfully synthesized at 1 GPa pressure by HPHT method. The microstructures and thermoelectric properties, such as Seebeck coefficient, electrical

*E-mail: maha@jlu.edu.cn

resistivity, and thermal conductivity have been researched carefully.

2. Experimental

Appropriate amounts of Co (99.95 %, 200 mesh), Sb (99.99 %, 200 mesh), Ni (99.5 %, 200 mesh), Fe (99.95 %, 200 mesh) were weighed according to the stoichiometry of $Ni_{0.15}Co_{3.85}Sb_{12}$ and $Fe_{0.2}Ni_{0.15}Co_{3.65}Sb_{12}$. The raw materials were homogeneously mixed in a glove box in the nitrogen gas atmosphere to avoid oxidation of cobalt element. The mixtures were cold-pressed into bulk disks ($\Phi = 10 \text{ mm} \times 3.5 \text{ mm}$) as precursors for HPHT synthesis. Then, the cylindrical disk was subjected to HPHT conditions for 25 min in a China-type large volume cubic high-pressure apparatus (CHPA) (SPD-6 \times 1200). The synthesis temperature (900 K to 920 K) was measured using a Pt-Rh 30 % Pt-Rh 6% B-type thermocouple, which was embedded near the sample. The synthesized samples were cut and polished for thermoelectric properties measurement.

The phase composition was characterized by X-ray diffraction (XRD) (D/MAX-RA) using $CuK\alpha$ ($\lambda = 1.5418 \text{ \AA}$) radiation in the 2θ range of 20° to 80° . The microstructures of the synthesized samples were examined by the field emission scanning electron microscopes (JEOL, JSM-6700F) and high-resolution transmission electron microscopy (JEOL, JEM-2200FS). The Seebeck coefficient and electrical resistivity were measured from 300 K to 700 K with a commercial equipment ZEM-3 (Ulvac-Riko). The thermal diffusivity λ was directly measured by the laser flash method with a commercial system (Netzsch LFA-427). The specific heat C_p measurement by DSC method was carried out using Linseis STA PT-1750 equipment with the standard sample (sapphire). The volume density d was measured by the Archimedes method. The total thermal conductivity κ was calculated as:

$$\kappa = \lambda C_p d \quad (2)$$

where λ , C_p , and d represent thermal diffusivity coefficient, specific heat capacity, and volume density, respectively.

3. Results and discussion

3.1. XRD spectra and optical images

The crystallographic structure of the synthesized samples can be identified by XRD patterns. From Fig. 1, we can see that all the diffraction peaks for $Ni_{0.15}Co_{3.85}Sb_{12}$ and $Fe_{0.2}Ni_{0.15}Co_{3.65}Sb_{12}$ are indexed as $CoSb_3$ structure (PDF# 98-976) [14]. No other diffraction peaks are present in the samples. All the samples crystallized in a body-centered-cubic structure with the space group of $Im\bar{3}$. The results show that polycrystalline $Ni_{0.15}Co_{3.85}Sb_{12}$ and $Fe_{0.2}Ni_{0.15}Co_{3.65}Sb_{12}$ samples have been successfully synthesized by HPHT method.

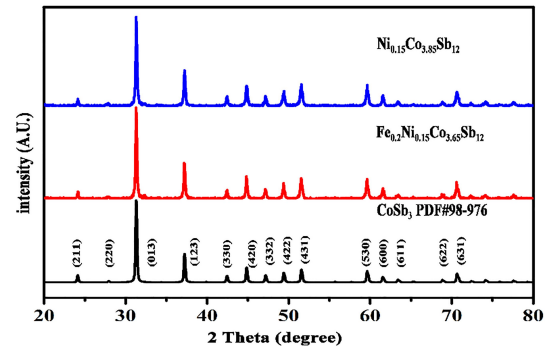


Fig. 1. XRD patterns of $Ni_{0.15}Co_{3.85}Sb_{12}$ and $Fe_{0.2}Ni_{0.15}Co_{3.65}Sb_{12}$ synthesized at 1 GPa by HPHT.

3.2. FESEM micrographs

Fig. 2 shows the fractured surfaces of $Ni_{0.15}Co_{3.85}Sb_{12}$ and $Fe_{0.2}Ni_{0.15}Co_{3.65}Sb_{12}$ samples synthesized at 1 GPa by HPHT. From Fig. 2, we can see that typical granulated grains with the size of the order of micrometers are tightly condensed. Particle morphology implies the isotropic crystal growth due to its cubic lattice structure. In addition, the grain boundaries of the samples are distinctly obvious. This is helpful in strengthening the phonon scattering, resulting eventually in the decrease of the lattice thermal conductivity [15]. The FESEM images also show that the average crystal particle size of $Fe_{0.2}Ni_{0.15}Co_{3.65}Sb_{12}$ is larger than that of $Ni_{0.15}Co_{3.85}Sb_{12}$.

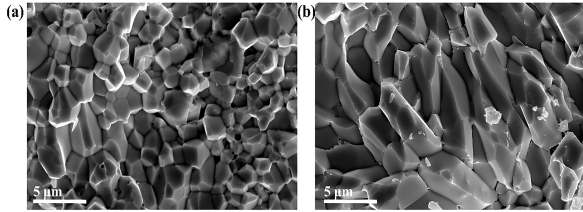


Fig. 2. FESEM micrographs of (a) $\text{Ni}_{0.15}\text{Co}_{3.85}\text{Sb}_{12}$ and (b) $\text{Fe}_{0.2}\text{Ni}_{0.15}\text{Co}_{3.65}\text{Sb}_{12}$ synthesized by HPHT.

3.3. HR-TEM micrographs

Fig. 3 shows the HRTEM micrographs of $\text{Ni}_{0.15}\text{Co}_{3.85}\text{Sb}_{12}$ and $\text{Fe}_{0.2}\text{Ni}_{0.15}\text{Co}_{3.65}\text{Sb}_{12}$ synthesized at 1 GPa by HPHT. Firstly, the distinct grain boundaries in the HRTEM images demonstrate the good crystallinity inside each individual grain. Secondly, Fig. 3a shows lattice deformations embedded inside the matrix, which is attributed to squeezing and twisting by stress. From Fig. 3b, we can see that the numerous lattice distortions, fringes, and defects exist in our samples, which is mainly caused by Fe substituting for Co on the basis of $\text{Ni}_{0.15}\text{Co}_{3.85}\text{Sb}_{12}$ [16]. We assume that the typical microstructures can enhance the phonon scattering, which further decreases the thermal conductivity to some degree [17].

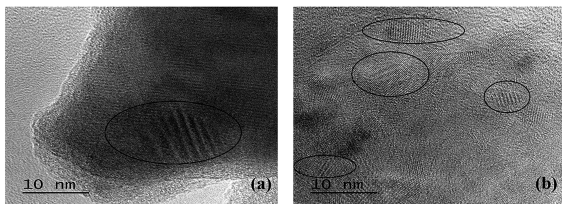


Fig. 3. HRTEM image of (a) $\text{Ni}_{0.15}\text{Co}_{3.85}\text{Sb}_{12}$ and (b) $\text{Fe}_{0.2}\text{Ni}_{0.15}\text{Co}_{3.65}\text{Sb}_{12}$ synthesized by HPHT.

3.4. Thermoelectric properties

The temperature dependence of the Seebeck coefficient is presented in Fig. 4a. The negative Seebeck coefficients indicate typical n-type transport behavior. As we can see, the absolute value of Seebeck coefficient of $\text{Ni}_{0.15}\text{Co}_{3.85}\text{Sb}_{12}$ and $\text{Fe}_{0.2}\text{Ni}_{0.15}\text{Co}_{3.65}\text{Sb}_{12}$ firstly increases with

increasing temperature, reaches a maximum of $238 \mu\text{V}\cdot\text{K}^{-1}$ and $180 \mu\text{V}\cdot\text{K}^{-1}$ at 600 K, respectively, and then decreases with the increase of temperature. Further, the absolute Seebeck coefficient of $\text{Fe}_{0.2}\text{Ni}_{0.15}\text{Co}_{3.65}\text{Sb}_{12}$ is lower than that of $\text{Ni}_{0.15}\text{Co}_{3.85}\text{Sb}_{12}$ at the whole measured temperature range, which is possibly attributed to the increased carrier concentration after Fe substituting for Co [18]. The relationship between the electrical resistivity and temperature is presented in Fig. 4b. It is clear that the electrical resistivity of $\text{Fe}_{0.2}\text{Ni}_{0.15}\text{Co}_{3.65}\text{Sb}_{12}$ sample increases with increasing temperature and then decreases above 650 K. However, the variation of electrical resistivity with temperature for the $\text{Fe}_{0.2}\text{Ni}_{0.15}\text{Co}_{3.65}\text{Sb}_{12}$ sample is very slight from $2.14 \text{ m}\Omega\cdot\text{cm}$ to $2.23 \text{ m}\Omega\cdot\text{cm}$ at this temperature range. Furthermore, the electrical resistivity of $\text{Ni}_{0.15}\text{Co}_{3.85}\text{Sb}_{12}$ sample decreases with increasing temperature, which is in agreement with the result presented in the literature [19].

Power factor (PF) is calculated from the measured Seebeck coefficient and electrical resistivity according to the following formula:

$$PF = S^2/\rho \quad (3)$$

As shown in Fig. 4c, $\text{Fe}_{0.2}\text{Ni}_{0.15}\text{Co}_{3.65}\text{Sb}_{12}$ sample yields a lower power factor values of $6.7 \times 10^{-4} \text{ W}\cdot\text{m}^{-1}\cdot\text{K}^{-2}$ after Fe substituting for Co site at room temperature. Further, $\text{Ni}_{0.15}\text{Co}_{3.85}\text{Sb}_{12}$ sample reaches the maximum power factor values of $25.80 \times 10^{-4} \text{ W}\cdot\text{m}^{-1}\cdot\text{K}^{-2}$ at 600 K. PF of $\text{Fe}_{0.2}\text{Ni}_{0.15}\text{Co}_{3.65}\text{Sb}_{12}$ sample reaches the maximum value of $14.76 \times 10^{-4} \text{ W}\cdot\text{m}^{-1}\cdot\text{K}^{-2}$ at 700 K. This is primarily attributed to the higher absolute value of Seebeck coefficient of $\text{Ni}_{0.15}\text{Co}_{3.85}\text{Sb}_{12}$.

The relationship between thermal conductivity and temperature is plotted in Fig. 4d. The thermal conductivities of both the samples decrease with the increasing temperature in the range of 300 K to 600 K. The minimum thermal conductivity values of $\text{Ni}_{0.15}\text{Co}_{3.85}\text{Sb}_{12}$ and $\text{Fe}_{0.2}\text{Ni}_{0.15}\text{Co}_{3.65}$ are $2.9 \text{ W}\cdot\text{m}^{-1}\cdot\text{K}^{-2}$ at 600 K and $2.8 \text{ W}\cdot\text{m}^{-1}\cdot\text{K}^{-2}$ at 700 K respectively, which can result from the intensified phonon scattering with temperature increase [20]. From Fig. 4d,

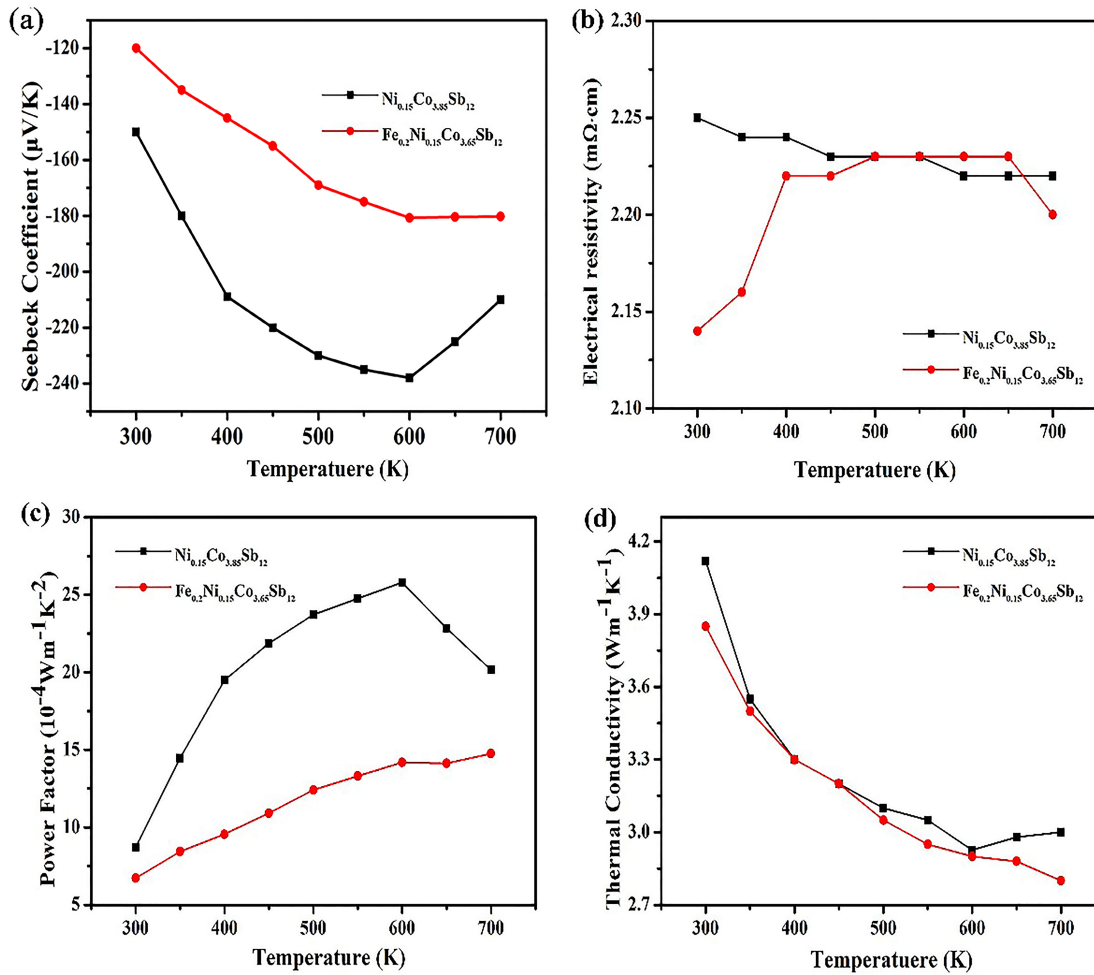


Fig. 4. Temperature dependence of (a) Seebeck coefficient, (b) electrical resistivity, (c) power factor and (d) thermal conductivity of $\text{Ni}_{0.15}\text{Co}_{3.85}\text{Sb}_{12}$ and $\text{Fe}_{0.2}\text{Ni}_{0.15}\text{Co}_{3.65}\text{Sb}_{12}$ samples.

we can see that thermal conductivity of $\text{Fe}_{0.2}\text{Ni}_{0.15}\text{Co}_{3.65}\text{Sb}_{12}$ sample is slightly lower than that of $\text{Ni}_{0.15}\text{Co}_{3.85}\text{Sb}_{12}$, which is attributed to Fe substituting for Co site that leads to the internal nature change [21].

Fig. 5 shows that temperature dependence of the figure-of-merit zT ($zT = S^2\sigma T/\kappa$) results from the measured values of the Seebeck coefficient, electrical resistivity, and thermal conductivity. The zT values of all samples increase firstly with increasing temperature, but zT values of $\text{Ni}_{0.15}\text{Co}_{3.85}\text{Sb}_{12}$ decrease with increasing temperature above 600 K, thus, the sample of $\text{Ni}_{0.15}\text{Co}_{3.85}\text{Sb}_{12}$

reaches the maximum zT value of 0.52 at 600 K. However, zT value of $\text{Fe}_{0.2}\text{Ni}_{0.15}\text{Co}_{3.65}\text{Sb}_{12}$ sample increases consistently with increasing temperature. A maximum zT value of 0.35 is achieved for $\text{Fe}_{0.2}\text{Ni}_{0.15}\text{Co}_{3.65}\text{Sb}_{12}$ at 700 K.

4. Conclusions

N-type single phase polycrystalline skutterudite compounds $\text{Ni}_{0.15}\text{Co}_{3.85}\text{Sb}_{12}$ and $\text{Fe}_{0.2}\text{Ni}_{0.15}\text{Co}_{3.65}\text{Sb}_{12}$ were successfully synthesized by HPHT method at 1 GPa in 25 min. We have carefully studied the microstructures

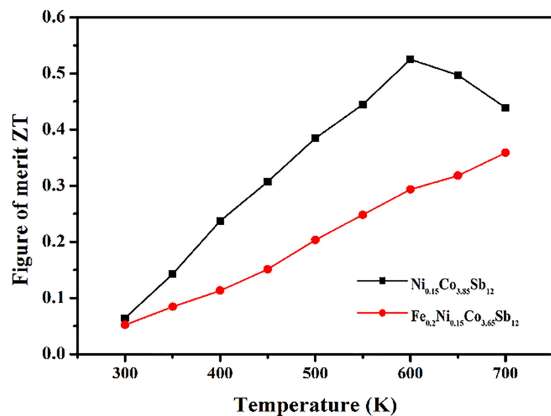


Fig. 5. Temperature dependence of figure-of-merit zT for $\text{Ni}_{0.15}\text{Co}_{3.85}\text{Sb}_{12}$ and $\text{Fe}_{0.2}\text{Ni}_{0.15}\text{Co}_{3.65}\text{Sb}_{12}$ samples.

and thermoelectric properties of the samples. A small amount of Ni-substituting skutterudite for Co sites yielded an improved thermoelectric performance. A maximum zT value of 0.52 was attained for $\text{Ni}_{0.15}\text{Co}_{3.85}\text{Sb}_{12}$ at 600 K. Although the maximum zT value of 0.35 for $\text{Fe}_{0.2}\text{Ni}_{0.15}\text{Co}_{3.65}\text{Sb}_{12}$ is lower than that of $\text{Ni}_{0.15}\text{Co}_{3.85}\text{Sb}_{12}$ at 700 K, the relatively lower thermal conductivity of $\text{Fe}_{0.2}\text{Ni}_{0.15}\text{Co}_{3.65}\text{Sb}_{12}$ is promising for high-performance Co-substituted skutterudite thermoelectric materials. Therefore, the significantly enhanced zT values of Co-substituted skutterudite are advantageous for the development of high-quality thermoelectric materials by HPHT method [22].

Acknowledgements

This work was financially supported by the Project of Jilin Science and Technology Development Plan (20170101045) and the Open Project of State Key Laboratory of Superhard Materials (Jilin University, No. 201609). The Project No. 2016065 Supported by the Graduate Innovation Fund of Jilin University.

References

[1] VENKATASUBRAMANIAN R., SIVOLA E., COLPITTS T., O'QUINN B., *Nature*, 413 (2001), 597.
 [2] RULL-BRAVO M., MOURE A., FERNÁNDEZ J.F., MARTÍN-GONZÁLEZ M., *RSC Adv.*, 5 (2015), 41653.

[3] CAILLAT T., BORSHCHEVSKY A., FLEURIAL J.P., *J. Appl. Phys.*, 80 (1996), 4442.
 [4] MORELLI D.T., CAILLAT T., FLEURIAL J.P., BORSHCHEVSKY A., VANDERSANDE J., CHEN B., UHER C., *Phys. Rev. B*, 51 (1995), 9622.
 [5] KAWAHARADA Y., KUROSAKI K., UNO M., YAMANAKA S., *J. Alloy. Compd.*, 315 (2001), 193.
 [6] SLACK G.A., ROWE D.M., *CR C*, 407 (1995).
 [7] LI Y.D., ZHENG Z.H., FAN P., LUO J.T., LIANG G.X., HUANG B.X., *Mater. Sci. Forum*, 847 (2016), 143.
 [8] WOJCIECHOWSKI K.T., TOBOLA J., LESZCZYŃSKI J., *J. Alloy. Compd.*, 361 (2003), 19.
 [9] KIM I.H., UR S.C., *Mater. Lett.*, 61 (2007), 2446.
 [10] NOLAS G.S., SLACK G.A., MORELLI D.T., TRITT T.M., EHRLICH A.C., *J. Appl. Phys.*, 79 (1996), 4002.
 [11] DENG L., JIA X.P., SU T.C., JIANG Y.P., ZHENG S.Z., GUO X., MA H.A., *Mater. Lett.*, 65 (2011), 1582.
 [12] ZHANG Y., JIA X., SUN H., SUN B., LIU B., LIU H., KONG L., MA H., *J. Alloy. Compd.*, 667 (2016), 123.
 [13] KONG L., JIA X., SUN H., ZHANG Y., SUN B., LIU B., LIU H., LIU B., MA H., *J. Alloy. Compd.*, 697 (2017), 257.
 [14] WEE D., KOZINSKY B., MARZARI N., FORNARI M., *Phys. Rev. B*, 81 (2010), 045204.
 [15] YAN X., LIU W., WANG H., CHEN S., SHIOMI J., ESFARIANI K., WANG H., WANG D., CHEN G., REN Z., *Energ. Environ. Sci.*, 5 (2012), 7543.
 [16] SUN H., JIA X., LV P., DENG L., GUO X., ZHANG Y., SUN B., LIU B., MA H., *RSC Adv.*, 5 (2015), 61324.
 [17] BISWAS K., HE J., ZHANG Q., WANG G., UHER C., DRAVID V.P., KANATZIDIS M.G., *Nat. Chem.*, 3 (2011), 160.
 [18] GHARLEGHI A., CHU Y.H., LIN F.H., YANG Z.R., PAI Y.H., LIU C.J., *ACS Appl. Mater. Inter.*, 8 (2016), 5205.
 [19] ZHAO X.Y., XUN S., CHEN L.D., TANG X.F., *J. Inorg. Mater.*, 21 (2006), 392.
 [20] MINNICH A.J., DRESSELHAUS M.S., REN Z.F., CHEN G., *Energ. Environ. Sci.*, 2 (2009), 466.
 [21] BERTINI L., STIEWE C., TOPRAK M., WILLIAMS S., PLATZEK D., MROTZEK A., ZHANG Y., GATTI C., MÜLLER E., MUHAMMED M., ROWE M., *J. Appl. Phys.*, 93 (2003), 438.
 [22] SHARP J.W., JONES E.C., WILLIAMS R.K., MARTIN P.M., SALES B.C., *J. Appl. Phys.*, 78 (1995), 1013.

Received 2016-10-15

Accepted 2017-08-20